Molecular Biology of the Cell
Vol. 16, 2129–2138, May 2005

Quantitative Characterization of a Mitotic Cyclin Threshold Regulating Exit from Mitosis

Frederick R. Cross,* Lea Schroeder,* Martin Kruse,*† and Katherine C. Chen‡

*The Rockefeller University, New York, NY 10021; and ‡Department of Biology, Virginia Polytechnic Institute and State University, Blacksburg, VA 24061-0406

Submitted October 14, 2004; Accepted January 24, 2005
Monitoring Editor: Mark Solomon

Regulation of cyclin abundance is central to eukaryotic cell cycle control. Strong overexpression of mitotic cyclins is known to lock the system in mitosis, but the quantitative behavior of the control system as this threshold is approached has only been characterized in the in vitro *Xenopus* extract system. Here, we quantitate the threshold for mitotic block in budding yeast caused by constitutive overexpression of the mitotic cyclin Clb2. Near this threshold, the system displays marked loss of robustness, in that loss or even heterozygosity for some regulators becomes deleterious or lethal, even though complete loss of these regulators is tolerated at normal cyclin expression levels. Recently, we presented a quantitative kinetic model of the budding yeast cell cycle. Here, we use this model to generate biochemical predictions for Clb2 levels, asynchronous as well as through the cell cycle, as the Clb2 overexpression threshold is approached. The model predictions compare well with biochemical data, even though no data of this type were available during model generation. The loss of robustness of the Clb2 overexpressing system is also predicted by the model. These results provide strong confirmation of the model's predictive ability.

INTRODUCTION

The cell cycle is governed by a well-characterized but highly complex regulatory network. Interlocking circuits regulating transcription, phosphorylation, and proteolysis of activators and inhibitors yield a robust oscillatory system that drives cell cycle events such as DNA replication and cell division with high efficiency and fidelity. The biochemical oscillator controlling the cell cycle (Hara *et al*., 1980) is largely based on the cyclical proteolysis of cyclins, leading to oscillations in cyclin-dependent kinase (Cdk) activity (Evans *et al*., 1983; Murray and Kirschner, 1989; Murray *et al*., 1989). Cdk activity oscillations are probably essential for cell cycle control. This is because critical multistep processes, including DNA replication and spindle morphogenesis/disassembly, are controlled by Cdk activity positively at one step and negatively at another (Nasmyth, 1996; Stern and Nurse, 1996; Stillman, 1996; Zachariae *et al*., 1999; Diffley and Labib, 2002). This couples a single oscillation of Cdk activity with one complete execution of each process. Appropriate thresholds for Cdk regulation of these steps (Stern and Nurse, 1996; Iwabuchi *et al*., 2002) imply that oscillations of Cdk activity will yield replication of chromosomes alternating with segregation of these chromosomes into daughter cells.

The reliance of this system on cyclin oscillations, and the highly nonlinear nature of the controls involved, means that sharp thresholds may be expected (Novak and Tyson, 1993; Tyson *et al*., 1995; Ferrell, 2002). In the *Xenopus* extract system, there is a well defined threshold for induction of mitosis by cyclin; interestingly, the system demonstrates hysteresis, because the threshold of cyclin required to block mitotic exit was lower than the threshold to induce mitotic entry (Pomerening *et al*., 2003, Sha *et al*., 2003).

The complexity of the cell cycle regulatory machinery makes for a very nonlinear system, such that full understanding probably requires a computational approach as well as an experimental one. Indeed, the results on cyclin thresholds in *Xenopus* were interpreted in a mathematical framework explaining the observed hysteresis by positive feedback loops in a system of ordinary differential equations describing the interactions of cyclin B-cdc2, Wee1, and Cdc25 (Pomerening *et al*., 2003; Sha *et al*., 2003). The modeling approach has been extended to the budding yeast cell cycle (Chen *et al*., 2000, 2004; Cross 2003; Thornton *et al*., 2004). These models describe the behavior of many more molecular components (and therefore contain many more equations), and they also contain a large number of parameters, many of which have not been measured experimentally. The main constraint for model generation and parameter estimation is fitting the behavior of mutants (viable and inviable) in various components of the control system. The most recent model (Chen *et al*., 2004) accounts for >100 mutants, with only a few mutants unaccounted for. A problem, though, is that essentially all the available data were used in model construction, resulting in a lack of independent model verification. Here, we experimentally quantitate a cyclin threshold for regulating mitotic exit. We then derive quantitative model predictions on cyclin levels to compare to the experimental measurements. These comparisons provide an orthogonal, independent test of the computational model's validity.

MATERIALS AND METHODS

Yeast Strains

Strain construction was carried out by standard methods. All strains were in the W303 background. The integrating *GAL-CLB2*, *GAL-CLB2-db*, *GAL-CLB2-*

This article was published online ahead of print in *MBC in Press* (http://www.molbiolcell.org/cgi/doi/10.1091/mbc.E04–10–0897) on February 16, 2005.

† Present address: Bernhard-Nocht-Institute for Tropical Medicine, AG Wiese, Bernhard-Nocht-Strasse 74, 20359 Hamburg, Germany.

Address correspondence to: Frederick R. Cross (fcross@rockefeller.edu).

ken, and *GAL-CLB2-ken,db* constructs were described previously (Wäsch and Cross, 2002); the *db* and *ken* mutations remove the destruction box and the two KEN boxes of Clb2, respectively. The constructs were placed in an integrating vector and targeted to the endogenous *CLB2* locus by *Xba*I digestion. Construction of the 2× *GAL-SIC1 CLB2-ken,db* strain with mutant *CLB2* at the endogenous locus was as described previously (Wäsch and Cross, 2002). All integrants were characterized for copy number by Southern blot. Integrants with either one or two integrated copies were subsequently used in crosses to construct strains of different backgrounds with defined *GAL-CLB2* copy number insertions. (The "2× *GAL-CLB2*" integration when heterozygous to wild-type *CLB2* in a diploid strain had similar Clb2 expression levels to a diploid homozygous for [i.e., containing two copies of] the "1× *GAL-CLB2*" integration [our unpublished data], indicating that the two tandem copies each functioned similarly to a single copy.) *cdh1* and *sic1* null strains were obtained from A. Amon (Massachusetts Institute of Technology). *APC-A* (mutated in anaphase-promoting complex [APC] subunit Cdc16, Cdc23, and Cdc27 Cdk phosphorylation sites; Rudner and Murray, 2000) and *TUB1-GFP::HIS3* strains were obtained from A. Murray (Harvard University). *CDC10::GFP* was obtained from K. Lee (National Institutes of Health). The *CDC6-Δ2-49* allele in this background was described previously (Archambault *et al*., 2003).

Other Methods

Elutriation was carried out as described previously (Cross *et al*., 2002), except that 1-liter cultures at ~5 ×10^6 cells/ml in YEP-raffinose were induced with 3% galactose for 2 h before harvesting and elutriation. Protein extraction and quantitative Western blotting were carried out as described previously (Cross *et al*., 2002). Preparation of Clb2-ken,db expressed from the endogenous promoter was carried out by shifting a 2× *GAL-SIC1 CLB2-ken,db* strain from galactose to glucose medium to shut off *GAL-SIC1* and to allow depletion of overexpressed Sic1 protein. After 0.5 h, cultures were elutriated, and fractions were harvested with small buds (from mid-cell cycle). These fractions were reinoculated in glucose medium and further incubated for 2 h. Western blotting for Clb2 showed an essentially constant concentration of Clb2-ken,db throughout the time course in these cells, which by the end of the time course were arrested in late mitosis as indicated by 2C DNA content, large buds, and divided nuclei (our unpublished data). Time-lapse microscopy was performed as follows: diploid strains containing a single copy of *TUB1-GFP* and *CDC10-GFP* were grown in complete synthetic raffinose medium to log phase and induced with 3% galactose for 1 h. They were then sonicated and plated on thin agarose slabs containing complete synthetic galactose medium, overlaid with a coverslip, and placed on a microscope stage in a 30°C enclosure. Green fluorescent protein (GFP) was detected by fluorescence microscopy at 3-min intervals for 6 h. The microscopic method will be described in detail elsewhere (Bean, Siggia, and Cross, unpublished data). Movies were scored for the time of septin ring formation and breakdown by Cdc10 fluorescence; and for the time of appearance of a long spindle, reflecting anaphase, and spindle breakdown by Tub1 fluorescence. The mean and standard deviations are plotted. Owing to problems of focus or ambiguities of scoring, not all intervals could be scored in all cell cycles in the movies. Although the wild type (wt) and 1× *GAL-CLB2* movies were generally straightforward to score, cytological events in the 2× *GAL-CLB2* movie were more ambiguous. In these movies, some of the measurements were lower limits because many cells did not complete mitosis before the end of the movie. Furthermore, spindle breakdown in this strain was variable. Long spindles sometimes seemed to split into two half-spindles that remained long and then were variably degraded down to a small line or dot with asters. (We scored spindle breakdown as qualitatively a "significantly" shorter pair of half-spindles; if the spindle just split into two half-spindles, this was not scored as full breakdown.) Ring breakdown in this strain also was unusually slow and partial (frequently two half-rings slowly dimmed). However, these scoring ambiguities do not affect the conclusion of mitotic exit defects specific to the 2× *GAL-CLB2* strain. Movies are available on request (fcross@rockefeller.edu).

Computation

Model predictions based on the Chen *et al*. (2004) model were carried out using WinPP software and code implementing the model (code and details available on request from Cross). Determination of a range of parameter values describing expression of *CLB2* from the *GAL* promoter ("ksb2-gal") was carried out using the model as described in the text. Note that all computations and experiments refer to the *GAL* promoter at single copy (or double copy for 2× *GAL-CLB2*) in diploid cells. Tests of ksb2-gal tolerance in models of heterozygous backgrounds (see text) were done using "daughter" parameters; "mother" parameters gave similar results shifted to slightly lower values (our unpublished data). In the model, for wild-type Clb2 protein, the rate constant for Cdh1-dependent degradation (which depends on the presence of both destruction box and KEN boxes) was kdb2″ = 0.4; and the rate constant for Cdc20-dependent degradation (which depends on the presence of destruction box only) was kdb2p = 0.15. For simulation of mutants with deleted proteolytic signals, the following rate constants for degradation of mutated Clb2 were assigned, based on Wäsch and Cross (2002): for Clb2 protein with destruction box deleted (Clb2-db), kdb2″ = 0.03 and kdb2p = 0; for Clb2 protein with KEN box deleted (Clb2-ken), kdb2″ = 0.03 and kdb2p = 0.15; and for Clb2 protein with both destruction box and KEN boxes deleted (Clb2-db,ken), kdb2″ = 0 and kdb2p = 0.

The Boolean network of Li *et al*. (2004) was modified to model constitutive *CLB2* expression: to equation 1 of Li *et al*. (2004) we added a constant "c" to the $\Sigma(a_{ij}{}^*S_j(t))$ for the Clb2 node (j = 10). This increases positive input into the Clb2 node at each time step (Matlab code available on request from Cross).

RESULTS

Cell Cycle Inhibition by Overexpression of the Mitotic Cyclin Clb2

The Clb2 mitotic cyclin must oscillate from a low level permissive for mitotic exit and replication origin reloading to a high level sufficient to drive entry into mitosis. A complex web of interlocking controls involving proteolysis, regulated transcription, and inhibitor accumulation controls Clb2 activity, and Clb2 reciprocally affects all of these regulators, making the final result of Clb2 overexpression difficult to predict intuitively. It is known that strong overexpression of *CLB2* RNA from the *GAL1* promoter (unregulated through the cell cycle) from multiple copies of *GAL-CLB2* causes mitotic arrest (Surana *et al*., 1993). We determined that in diploid cells, our *GAL-CLB2* construct resulted in viable cells with close to wild-type proliferation rate when present at single copy ("1× "), but this construct efficiently blocked proliferation when present at two copies ("2× "; a tandem duplicated array of *GAL-CLB2*) (Figure 1). The 1× *GAL-CLB2* construct blocked proliferation in haploids almost as well as the 2× *GAL-CLB2* construct did in diploids in the same assay (our unpublished data). Also, similar inhibition was observed in diploid cells containing 2× *GAL-CLB2* on one chromosome as for diploid cells containing two copies of a chromosome containing 1× *GAL-CLB2* (our unpublished data). These results indicate that proliferation is inhibited at a dosage of two copies of the *GAL-CLB2* construct per diploid genome but not by one copy.

The precipitous decline in proliferation capacity with a simple doubling of gene dosage suggests the crossing of a threshold. Consistent with this, we found that 1× *GAL-CLB2* diploid strains had an absolute requirement for *CDH1* and *SIC1* for viability, unlike wild type, suggesting that the 1× *GAL-CLB2* cells were only viable conditional on the full activation of the normally dispensable Cdh1-Sic1 control system. Indeed, 1× *GAL-CLB2* diploid strains exhibited significant slowing of proliferation just upon a halving of *CDH1* gene dosage (Figure 1), and a weaker but detectable effect was observed upon halving of *SIC1* gene dosage, which was significantly enhanced on removal of the Cdk-inhibitory N-terminal domain of Cdc6 (Figure 1). This domain of Cdc6 was shown previously to play an ancillary role in regulating mitotic exit, perhaps by binding to and inhibiting Clb2 (Archambault *et al*., 2003).

In addition, the viability of 1× *GAL-CLB2* diploids is completely dependent on the phosphorylation of APC subunits. These phosphorylations were previously implicated as required for full activity of the Cdc20-APC (Rudner and Murray 2000, Cross 2003). Even heterozygosity for the unphosphorylatable APC mutations has a slight effect on proliferation of these cells (Figure 1). Therefore, we conclude that the 1× *GAL-CLB2* diploids are just under a threshold for inviability due to Clb2 overexpression, whereas the 2× *GAL-CLB2* diploids are just over this threshold. The level of this threshold is set by the combined activities of APC-Cdc20, APC-Cdh1, and Sic1.

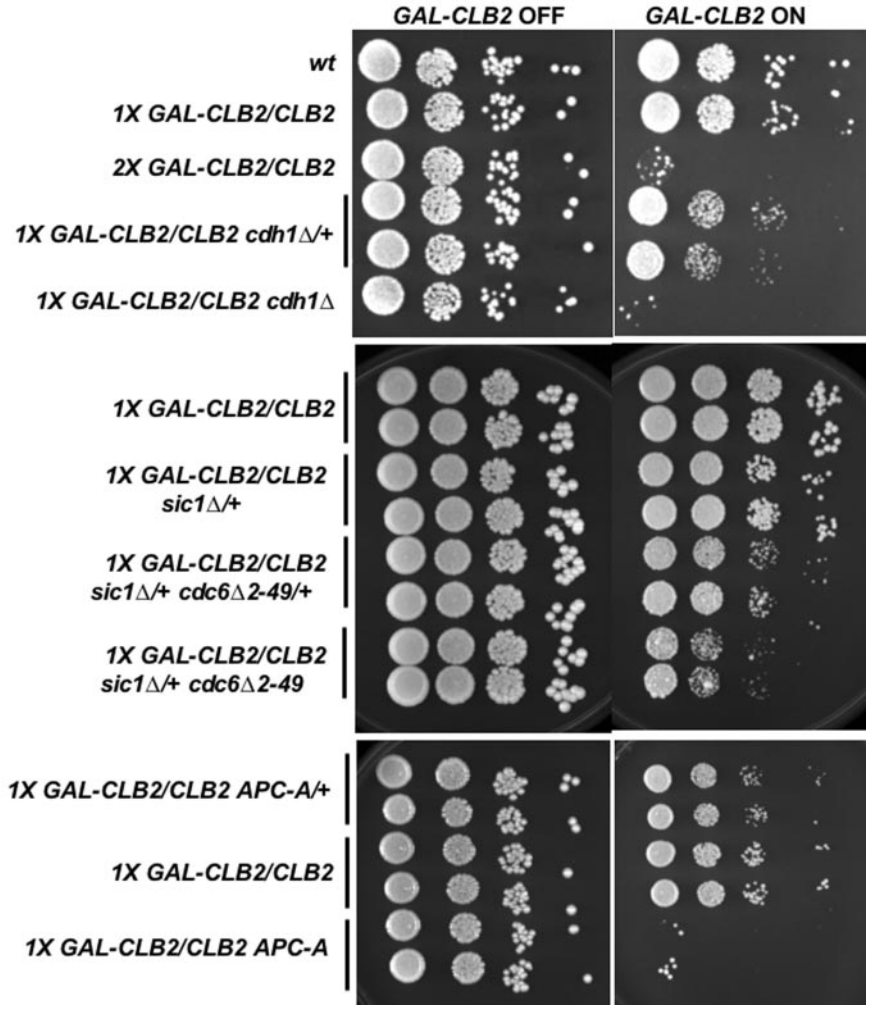

Figure 1. Dosage sensitivity for *CLB2* overexpression. Tenfold serial dilutions of fresh stationary phase cultures of diploids of the indicated genotypes were plated on YEPD or YEP-galactose. Genotype nomenclature: *1× GAL-CLB2/CLB2* means one copy of *GAL-CLB2* integrated at the *CLB2* locus, heterozygous with a normal *CLB2* locus; 2× is the same but with two tandem copies of *GAL-CLB2*. *cdh1*Δ/+ means heterozygosity for a *cdh1* deletion; *cdh1*Δ means homozygosity for the deletion. *APC-A*/+ refers to the presence of mutations blocking Cdk phosphorylation of Cdc16, 23, and 27 (Rudner and Murray, 2000) in one allele of *CDC16*, *CDC23*, and *CDC27*, heterozygous with a wild-type allele of each; *APC-A* is homozygous for these mutations in all three genes. Top, dosage sensitivity for *GAL-CLB2* and interaction with *CDH1* dosage. Middle, interaction with *SIC1* dosage. Bottom, interaction with *APC-A* mutations.

Characterization of Mitotic Defects in Clb2 Overexpressors by Time-Lapse Microscopy

The 2× *GAL-CLB2* cells accumulated as predominantly large-budded, binucleate cells in liquid medium (our unpublished data). To characterize the mitotic defect in these cells more carefully, we examined wild-type control, 1× *GAL-CLB2*, and 2× *GAL-CLB2* cells by time-lapse microscopy, in cells containing GFP-labeled tubulin and septin rings (derived from *TUB1-GFP* and *CDC10-GFP*) (Figure 2). These markers allow clear determination of the timing of septin ring formation (indicative of cell cycle Start), spindle elongation (indicative of entry into mitosis and anaphase), and events characteristic of mitotic exit: spindle breakdown and septin ring breakdown. Although the wild-type control and 1× *GAL-CLB2* cells displayed similar cell cycle kinetics as determined by these markers, the 2× *GAL-CLB2* cells exhibited strong delays specifically in the spindle elongation–spindle breakdown interval and the spindle breakdown–septin ring breakdown interval (Figure 2C). These results indicate a specific delay or arrest in mitotic exit. The response was not uniform, with some cells exhibiting long delays and others blocking for the 6-h duration of the movie. These data indicate that the 2× *GAL-CLB2* cells block or delay mitotic exit and have the further interesting implication that different events in mitotic exit may have different thresholds for inhibition by Clb2 (see *Materials and Methods* for a full description).

A general question in this experimental design is whether the results are due to saturation of the ubiquitination or proteolysis machinery by overexpression or due to specific regulatory interactions below saturation. We have no direct information bearing on this issue. However, the movies suggest that formation of the long telophase spindle occurs approximately on schedule after septin ring formation in all three strains. Because spindle elongation requires APC-dependent and proteosome-dependent Pds1 removal to allow cohesin cleavage (Zachariae and Nasmyth, 1999), this suggests that the APC and proteosome are not grossly saturated in the 2× *GAL-CLB2* strain.

Quantitation of Levels of Clb2 upon Overexpression

We used the quantitative Western blotting method described previously (Cross *et al.*, 2002) to measure the number of Clb2 proteins per cell in diploid cells that were wild type, 1× *GAL-CLB2*, or 2× *GAL-CLB2*. The results (Table 1) indicated an average level of 1500 Clb2 molecules per cell in wild-type cycling cells (consistent within experimental error with our previous estimate of 1100). The 1× *GAL-CLB2* construct resulted in a fivefold increase and the 2× *GAL-CLB2* in a 13-fold increase (note that in the latter construct, this number represents cells that are strongly delayed or arrested in mitosis and thus has a different interpretation from the asynchronous average measurements for WT and 1× *GAL-CLB2*).

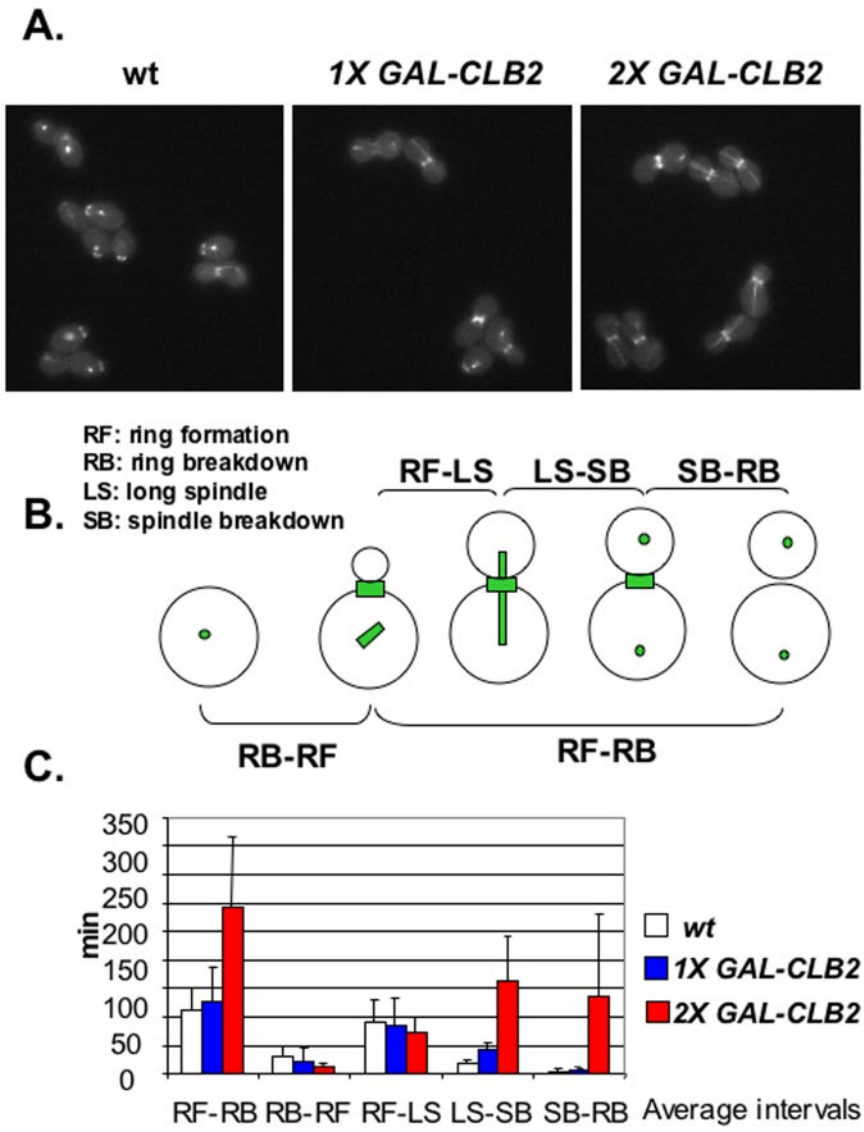

Figure 2. Time-lapse microscopy analysis of *CLB2* overexpressors. Wild-type *CLB2/CLB2*, 1× *GAL-CLB2/CLB2*, and 2× *GAL-CLB2/CLB2* strains, all containing a copy of *TUB1-GFP* and *CDC10-GFP*, were grown to log phase in Sc-raffinose medium, preinduced with galactose for 1 h, and then plated on Sc-galactose slabs. Time-lapse microscopy was carried out for 6 h with GFP detection every 3 min. (A) Still images from the 3-h time point. (B) Cartoon of the cell cycle with septin ring (collar between cell and bud, labeled by Cdc10-GFP) and spindle (dot and line, labeled by Tub1-GFP), with the relevant intervals indicated. (C) Approximate quantitation of cell cycle intervals for all scoreable cells in the movies, mean and SD. See *Materials and Methods* for more information on scoring.

Dynamic Range of Overexpressed Clb2 through the Cell Cycle

The measurements reported above were from cultures that were not synchronized before harvesting. The known strong periodicity of Clb2 means that such measurements are averages over a considerable amount of variation. To determine the dynamic behavior, we performed centrifugal elutriation to isolate small newborn cells known to contain the minimum level of Clb2 because of completion of proteolysis during exit from the previous mitosis and large cells from mid-cycle that contain the peak level of Clb2. We carried this experiment out with wild-type diploid cells and with diploid cells containing one or two copies of *GAL-CLB2*. Because constitutive induction of the 2× *GAL-CLB2* construct strongly delayed mitotic exit, we induced with galactose in these experiments for just the minimum time (2 h) required for full induction of Clb2 from the *GAL-CLB2* construct (our unpublished data). The wild-type and 1× *GAL-CLB2* cells were taken through an identical galactose induction.

The results (Figure 3) showed that wild-type cells exhibited a large-amplitude regulation of Clb2 levels, as expected, with peak levels occurring in cells of a size where most had budded and completed replication, and nuclear division was beginning. The 1× *GAL-CLB2* cells showed a similar correlation of budding, DNA replication, and nuclear division with cell size, although the trough level of Clb2 was clearly considerably higher than that in wild-type cells. The 2× *GAL-CLB2* cells, even after the minimum 2-h galactose induction, demonstrated a general shift of the population to large-volume budded cells that had completed DNA replication, and the proportion of binucleate cells rose to the majority in the larger cell size fractions. Clb2 protein was high throughout the fractions, although some regulation in the smaller versus the larger cells was apparent. Although it seems paradoxical to recover any smaller daughter cells with Clb2 overexpression sufficient to inhibit mitotic exit, we induced with galactose for the minimum time to avoid this problem, and in addition, as shown above by time-lapse microscopy, the overexpressor is somewhat leaky, and new daughters continue to be produced at a low rate.

To directly compare the Clb2 levels in fractions from the different elutriations, we used Western blotting to the Pgk1 protein to standardize protein levels loaded and directly compared Clb2 levels at the troughs and peaks of the vari-

Table 1. Left, asynchronous Clb2 concentrations quantitated by serial-dilution Western blotting by using MBP-Clb2 as a recombinant standard, as described previously (Cross *et al*., 2002), in diploid strains containing zero, one, or two copies of a *GAL-CLB2* integrated construct, in addition to two copies of the wild-type *CLB2* gene

Experiment	Copies/cell, mean ± SEM (fold increase over wt)	Model ksb2-gal (Clb2 au/min)	Model Clb2 concentration (Clb2 au/cell mass, relative to wt)
Wt	1500 ± 461	0.001	1
1× GAL-CLB2	7400 ± 1081 (5× wt)	0.32–0.48	5–7
2× GAL-CLB2	19,000 ± 2985 (13× wt)	0.64–0.96	7–34

Cultures were grown to log phase in YEP-raffinose medium and induced for 3 h by addition of 3% galactose. Mean ± SE of mean and fold increase from wild-type are shown. Right, simulations of Clb2 concentration (molecules in arbitrary units/cell mass, integrated through the computed cell cycle) are shown for the wild type and 1× GAL-CLB2 cells. Due to predicted arrest with ksb2-gal = 0.64–0.96 for 2× GAL-CLB2 cells, the Clb2 concentration is calculated at 240 min, rather than integrating through the cell cycle. The results are not very sensitive to this time choice.

ous elutriations (Figure 4). We found that the peak level of Clb2 in wild-type cells is similar to the trough level in 1× *GAL-CLB2* cells, and the peak level in 1× *GAL-CLB2* cells is similar to the trough in 2× *GAL-CLB2* cells. Two replicates of this experiment are shown, with completely independent elutriations for all samples. An approximate quantitation of these data by densitometry indicated a greater than 10-fold Clb2 oscillation in wild-type comparing peak to trough, as expected; an approximately fivefold oscillation in the 1× *GAL-CLB2* strain; and an approximately two- to threefold variation in Clb2 levels across the fractionation in the 2× *GAL-CLB2* strain.

We also examined the behavior of 1× *GAL-CLB2* cells that were heterozygous for either *cdh1* or *sic1* deletion, in the same protocol. Interestingly, these cells showed significant deregulation of Clb2 levels in the trough fractions compared with the 1× *GAL-CLB2* controls, whereas the peak fractions were comparable. This result suggests that these cells, which are at the borderline of inviability due to Clb2 overexpression and weakening of the control system due to heterozygosity, leak through mitosis and enter the succeeding G_1 with significantly elevated Clb2 levels.

The 1× *GAL-CLB2* cells mutant for APC phosphorylation sites (Rudner and Murray, 2000) rapidly arrested upon galactose induction as large budded binucleate cells, and the elutriated culture showed high Clb2 levels in all size fractions (our unpublished data), consistent with a previous report (Cross 2003).

Comparison of Experimental Results to Computation

We wanted to compare the biochemical results mentioned above with predictions from the quantitative model of Chen *et al*. (2004) describing control of the yeast cell cycle. This model contains two parameters governing *CLB2* transcription. One (ksb2′, 0.001 au/min) is unregulated, basal expression. The other (ksb2″, 0.04 au/min) represents peak of regulated *CLB2* transcription rate from its endogenous promoter, regulated by the Mcm1/SFF complex. These rate constants have a unit of minutes^{-1}. Thus, the concentration of each protein is not expressed in absolute concentration (e.g., nanomolar), but rather, in "arbitrary units" (au). As discussed in Chen *et al*. (2004), the au for Clb2 can be calibrated from quantitations of asynchronous Clb2 levels (Cross *et al*., 2002) to yield an estimate of 1 au = 40 nM or 2400 molecules per diploid cell; ksb2″ = 0.04 would then correspond to ~100 molecules per minute per diploid cell.

Expression of *CLB2* from the *GAL* promoter is modeled by increasing ksb2′, because the *GAL* promoter is not cell cycle regulated. For clarity, we will name this modified ksb2′ parameter used to model *GAL-CLB2* "ksb2-gal." We asked whether there was a theoretical level of ksb2-gal that would allow mitotic exit, whereas a twofold increase in this value would block mitotic exit. To make this determination, the standard parameter set of Chen *et al*. (2004) was modified. First, mass-doubling-time was changed to 150 min (from 90 min) to reflect that cell growth is slower on galactose medium (this modification was used in Chen *et al*., 2004 to model all results on galactose medium). The ksb2′ (=ksb2-gal) parameter was then systematically increased, and the ability of both mother and daughter cells to cycle repetitively was tested. (Mother cells inherit a bigger fraction of the cell mass at cell division and are therefore predicted to be more sensitive to high expression of Clb2 than daughter cells; our unpublished data). At a value of ksb2-gal< = 0.48, both mother and daughter can cycle indefinitely. Values of ksb2-gal from 0.49 to 0.63 cause mother cells but not daughter cells to arrest in mitosis. Still higher values (ksb2-gal ≥ 0.64) cause both mother and daughter cells to arrest. Therefore, ksb2-gal = 0.48 is the maximum level for 1× *GAL-CLB2* to yield viable mothers and daughters, and ksb2-gal = 0.64 is the minimum level for 2× *GAL-CLB2* to yield inviable mothers and daughters. Thus, the predicted allowable range of ksb2-gal for the 1× *GAL-CLB2* strain is 0.32–0.48. Model runs are shown in Figure 5. With ksb2-gal = 0.35 (modeling 1× *GAL-CLB2*), cycling occurred normally although with very high Clb2 levels, whereas with ksb2-gal = 0.70 (2-fold higher, modeling 2× *GAL-CLB2*) the system arrested in the first cell cycle (Figure 5).

A caveat for this computation is that as was shown by time-lapse microscopy (Figure 2), the 2× *GAL-CLB2* cells do not uniformly arrest before mitotic exit but rather experience long but variable delays in events in mitotic exit; most cells ultimately do manage to divide and enter the succeeding cell cycle, in which they also exhibit variable delays. This kind of behavior probably reflects stochastic variation among the cells and therefore is not seen in the deterministic computational model. (This caveat might suggest ksb2-gal estimates at the lower end of the indicated range.)

A second caveat comes from the fact that "Clb2" in the model essentially represents the larger class of mitotic cyclins comprised by Clb1,2,3,4. Whereas Clb2 is both functionally the most significant and quantitatively the most abundant, Clb1,3,4 collectively are about as abundant as Clb2 (Cross *et al*., 2002). Considering Clb1,3,4 to be fully functionally equivalent to Clb2 is problematic, though, as discussed previously (Cross *et al*., 2002). Therefore, for the present

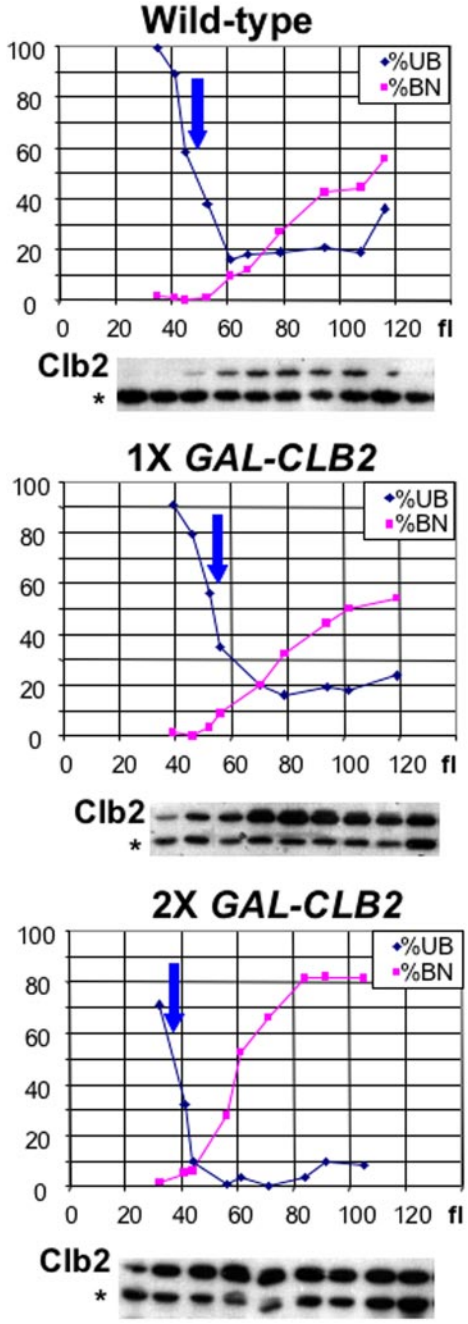

Figure 3. Clb2 levels through the cell cycle determined by elutriation. One-liter cultures of diploids that were wild-type *CLB2/CLB2*, 1× *GAL-CLB2/CLB2*, or 2× *GAL-CLB2/CLB2* were grown in YEP-raffinose, and induced for 2 h with 3% galactose. Cultures were collected by filtration, elutriated, and samples of increasing cell volume were collected and analyzed for percentage of unbudded cells (%UB, blue symbols), binucleate cells (%BN, pink symbols), and DNA content by fluorescence-activated cell sorting (fraction where ~50% of cells had completed replication indicated by blue arrow), plotted against the mode cell volume in the fractions, in femtoliters. Clb2 content in the fractions was determined by Western analysis. *, a nonspecific band in the anti-Clb2 Western blot. This band is an imperfect loading control for these blots because some Clb2 degradation products comigrate with this band, especially in the overproducers (our unpublished data); therefore, accurate comparison requires reference to another loading control such as the Pgk1 Western blot in Figure 4.

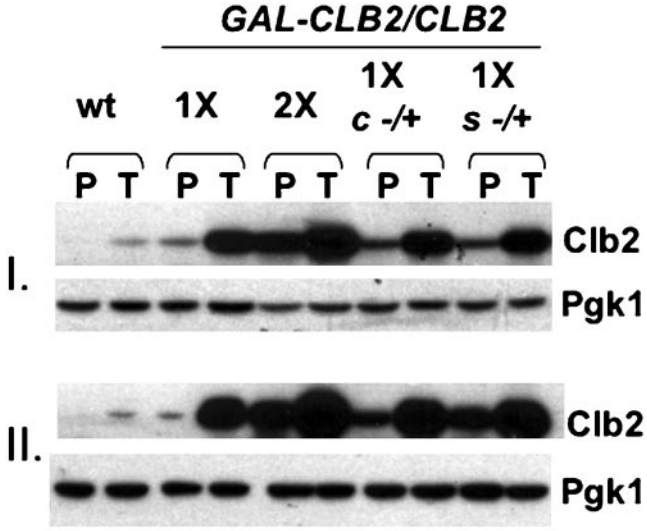

Figure 4. Comparison of trough and peak levels of Clb2 upon Clb2 overexpression. The lowest (trough, T) and highest (peak, P) Clb2 samples from elutriation experiments such as the ones shown in Figure 3 were run on the same gel. Equal loading was established by anti-Pgk1 Western blot, and the relative levels of Clb2 at peak and trough were determined by anti-Clb2 Western blot. Strains tested were wild-type *CLB2/CLB2*, 1× *GAL-CLB2/CLB2*, 2× *GAL-CLB2/CLB2*, 1× *GAL-CLB2/CLB2 cdh1/+*, and 1× *GAL-CLB2/CLB2 sic1/+*. Two replicates of the experiment are shown (I and II), with independent elutriations for all samples.

purposes, we continue to assume that Clb2 is the main significant activity for quantitative book-keeping. This idea is supported by a mitotic delay phenotype from deleting *CLB2*, and a significantly lesser phenotype even from simultaneously deleting *CLB1,3,4* (Fitch *et al*., 1992; our unpublished data).

Reduced viability of 1× *GAL-CLB2 sic1/+* (especially with the inhibitory effect of Cdc6 removed), *cdh1/+* and *APC-A/+* heterozygous strains (Figure 1) allows an independent test of the parameter estimation of ksb2-gal. Reducing the activity of Cdh1 toward Clb2 (kdb2″) by twofold resulted in predicted mitotic arrest with ksb2-gal of ≥ 0.38 (using the daughter cell parameters, where the standard parameter set could tolerate ksb2-gal up to 0.63; see above). Reducing the ability of Clb2 to phosphorylate and activate the APC (ka20″) by twofold resulted in predicted mitotic arrest with ksb2-gal of ≥0.46. Reducing the synthesis rate of *SIC1* in the model (ksc1′, ksc1″) by twofold resulted in predicted mitotic arrest with ksb2-gal of ≥0.49; simultaneously halving the synthesis rate of Cdc6 lowered this threshold to ≥0.26. These thresholds for the heterozygous backgrounds are approximately within the 0.32–0.48 range for the ksb2-gal parameter. Thus, the model predicts a transition from viability to inviability in these heterozygous backgrounds somewhere within this range of constitutive Clb2 expression. The reduced viability of these heterozygous backgrounds containing one copy of *GAL-CLB2* thus confirms by an independent set of genetic assays that this parameter range for the *GAL-CLB2* construct gives a reasonable fit between model and experiment. (The results also suggest choosing a value in the lower end of the range, because the heterozygous strains are all viable). Modeling *GAL-CLB2* expression with ksb2-gal anywhere in the 0.32–0.48 range predicts complete block to mitotic exit in homozygous *cdh1*, homozygous *APC-A* or *sic1/+ CDC6*Δ*2-*

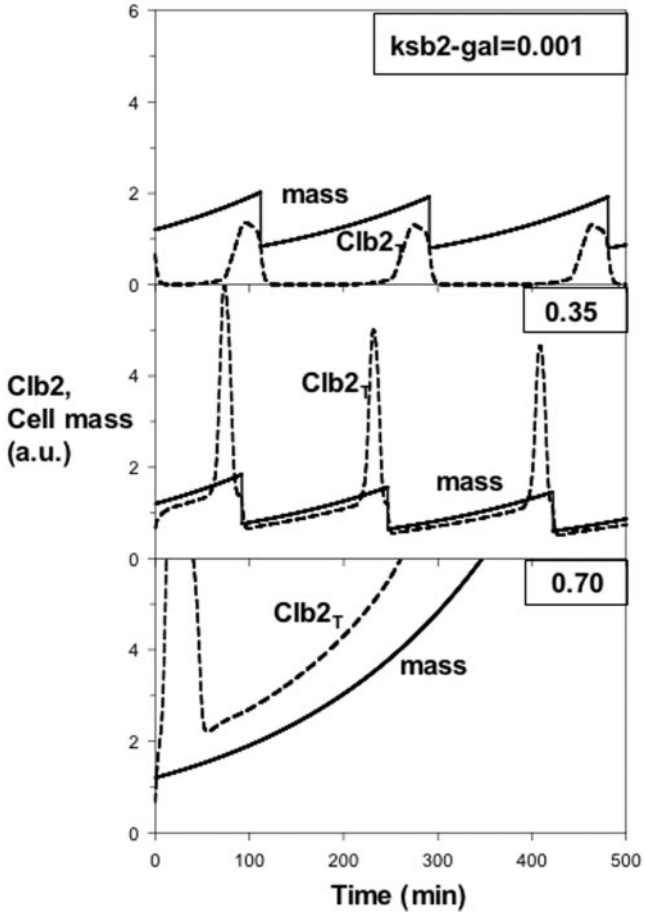

Figure 5. Model predictions. Clb2 levels and cell mass plots from the model for ksb2-gal = 0.001 (modeling wild-type; ksb2-gal substitutes for ksb2′ = 0.001 in the original model), ksb2-gal = 0.35 (in the estimated range for 1× *GAL-CLB2*), and ksb2-gal = 0.7 (in the estimated range for 2× *GAL-CLB2*). Clb2, cell mass units are arbitrary; as in Chen *et al.* (2004).

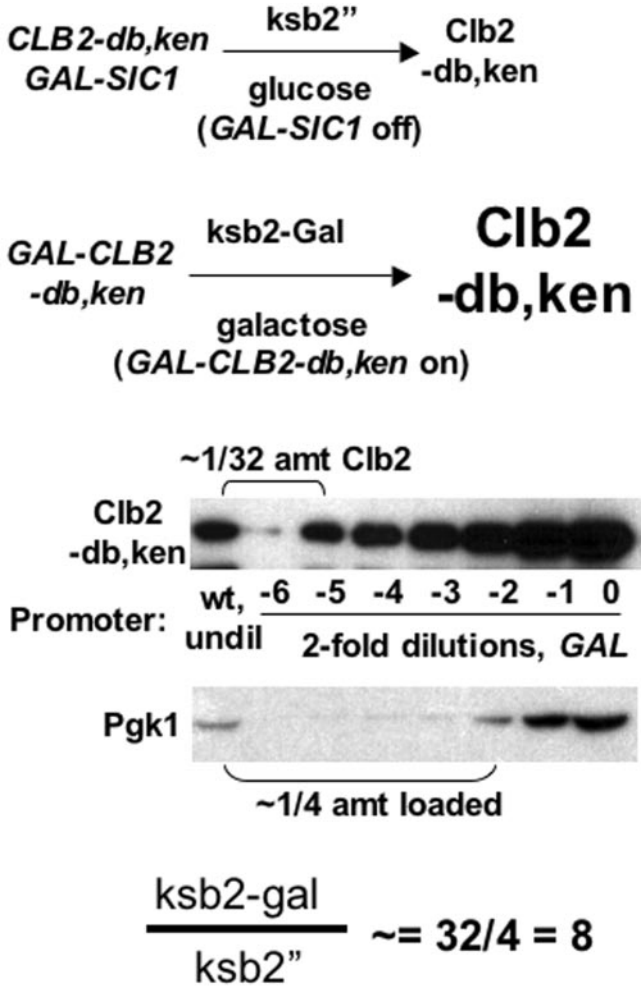

Figure 6. Accumulation of proteolytically resistant Clb2 from different promoters. Top, schematic diagram of the experimental design; the large font for *GAL-CLB2-ken,db* indicates that this is an overexpressor, but both overexpression and endogenous expression of Clb2-ken,db result in mitotic arrest (Wäsch and Cross, 2002; our unpublished data). Samples of protein from cells arrested in mitosis due to expression of Clb2-ken,db from the endogenous *CLB2* promoter were obtained using 2× *GAL-SIC1 CLB2-ken,db* (endogenous locus) (see *Materials and Methods*). Samples of protein from cells arrested in mitosis due to expression of Clb2-ken,db from the *GAL1* promoter were obtained by inducing a 1× *GAL-CLB2-ken,db* diploid strain with galactose for 3.5 h. Serial dilutions of the latter extract were run on gels together with the former extract run undiluted, and probed with anti-Clb2, and with anti-Pgk1 as a loading control. In this experiment, we estimate that approximately one-fourth the level of the endogenously expressing undiluted sample was loaded about compared with the *GAL* promoter sample based on Pgk1 staining, whereas the Clb2 comparison indicated an ~32-fold excess in the *GAL1* promoter sample. From this experiment, the estimated ratio of the two promoter strengths is thus 32/4 = 8. A second experiment gave an estimate of 16, for a log-average estimate of 11.

*49/CDC6*Δ*2-49* backgrounds, also consistent with experiment (Figure 1).

To determine whether the above-mentioned estimate for *GAL-CLB2* expression is biochemically accurate, we examined cells blocked for mitotic exit by undegradable Clb2, with the destruction box and KEN boxes mutated (Clb2-ken,db; Wäsch and Cross, 2002, Hendrickson *et al.*, 2001). We used either *CLB2-ken,db* expressed from the endogenous promoter (Wäsch and Cross, 2002) or from the *GAL* promoter at single copy (the identical construct to the 1× *GAL-CLB2* used described above, but with the *ken,db* mutations). Because Clb2-ken,db is immune to proteolytic regulation, the Clb2-ken,db levels can be used as a direct transcriptional activity readout. The Clb2 level in *CLB2-ken,db GAL-SIC1* cells blocked for mitotic exit by turning off *GAL-SIC1* (by incubating in glucose) should be proportional to ksb2″ (peak mitotic expression of *CLB2*), and the Clb2 level in *GAL-CLB2-ken,db* cells blocked for mitotic exit (by incubating in galactose) should be proportional to ksb2-gal (rate of expression from the *GAL* promoter). We compared these two levels by serial dilution in Western blotting experiments, standardizing by Pgk1 protein levels (Figure 6). We found that the *GAL-CLB2-ken,db* cells in galactose contained ~11-fold more Clb2 than *CLB2-ken,db GAL-SIC1* cells incubated in glucose. Thus, the estimate derived from this biochemical measurement for ksb2-gal is 11 times ksb2″ = 11× 0.04 = 0.44. This estimate is within the 0.32–0.48 range derived solely from the previous computational model and the biology of 1× versus 2× *GAL-CLB2* cells. Given the assumptions required for this calculation and the differences in the assay conditions (glucose shutoff of *GAL-SIC1* compared with galactose induction of *GAL-CLB2-ken,db*), we consider this result to be

good independent biochemical confirmation of the validity of the estimated range.

The equations we use assume that degradation of Clb2 is linearly proportional to the amount of Clb2, that is, we assume, the degradation machinery does not show saturation even at high concentration of the Clb2 substrate. Strictly speaking, this is certainly not correct. (The same problem occurs in the descriptions for the degradation of other regulatory elements in the model.) Thus, under conditions of strong Clb2 overexpression, we could be partially misattributing the cause of Clb2 to due specific regulatory interactions rather than to saturation of the degradation machinery. The agreement of experimental results with the model predictions gives us some confidence that saturation is probably not important in this context, but we cannot be certain of this.

This range of estimates for ksb2-gal then allows direct comparison between the model's predictions and the biochemical results in Table 1. We calculated the model's average concentration of Clb2 (in arbitrary units) in a cycling population of wild-type cells, and in cells modeling 1× or 2× *GAL-CLB2* (calculation described in Table 1 legend). These amounts, standardized to wild type, compared well to the experimental measurements (Table 1).

The critical point here is that the estimates for ksb2-gal used in these calculations were derived solely from consideration of how much this parameter could be increased before the model predicted inviability. Thus, it is a purely genetic prediction, standardized to the endogenous ksb2″ value of the model. Following this prediction, two independent biochemical measurements (the level of undegradable Clb2-ken,db from the wild-type *CLB2* promoter vs. the *GAL* promoter [Figure 6], and the level of Clb2 in unsynchronized wild-type, 1× and 2× *GAL-CLB2* cells [Table 1]) are shown to fit well with the estimate. Thus, these biochemical measurements represent an independent test of the model.

Model Predictions for Dynamic Behavior of Overexpressed Clb2 through the Cell Cycle

Figure 5 presents model runs demonstrating the difference in predicted dynamic behavior as basal *CLB2* RNA expression is increased through the threshold for blocking mitotic exit. A semiquantitative prediction can be made from these runs that in 1× *GAL-CLB2* cells, near the maximum tolerable level of *CLB2* overexpression, the trough level of Clb2 in G1 should correspond to the peak level of wild-type, whereas the peak level in the 1× *GAL-CLB2* cells should approximately correspond to the trough level in the 2× *GAL-CLB2* cells. These expectations are met by the experimental data (compare Figure 4 with Figure 5), although we did not attempt accurate measurement of all the samples from the elutriations to allow a quantitative comparison of the complete cell cycle profiles to the theoretical profiles in Figure 5.

Overexpression of Proteolysis-resistant Clb2

Clb2 proteolysis is highly complex, with Cdc20-dependent (also destruction-box-dependent) proteolysis dominating during mitosis and Cdh1-dependent (also destruction-box and KEN-box dependent) proteolysis dominating during G_1 (Wäsch and Cross, 2002). As a final test of the ability of the model to handle Clb2 overexpression, we quantitated the level of Clb2-db, Clb2-ken, and Clb2-ken,db from the *GAL* promoter, and compared the results to model predictions, by using the ksb2-gal range derived above (additional assumptions in *Materials and Methods*). A good agreement between model and experiment is observed (Table 2); this is striking considering *GAL-CLB2-ken,db* cells accumulate ~2 orders of magnitude higher levels of Clb2 than do wild-type cells.

Table 2. Accumulation of proteolysis-resistant versions of Clb2 from the *GAL* promoter

	Copies/cell, mean ± SEM (fold increase over wt)	Predicted fold increase over wt
wt	1500 ± 461	1
GAL-CLB2-wt	7400 ± 1081 (5× wt)	5–7
GAL-CLB2-db	49,000 ± 12,606 (33× wt)	39–57
GAL-CLB2-ken	18,000 ± 2019 (12× wt)	12–18
GAL-CLB2-ken,db	91,000 ± 19,557 (61× wt)	39–57

A wild-type diploid strain, or diploid strains with single integrations of the indicated *GAL-CLB2* construct were induced with galactose for 3 h, and Clb2 quantitated as described in Table 1. Model predictions were generated as in Table 1, assuming that Clb2-db was insensitive to APC-Cdc20 and reduced 13-fold in sensitivity to APC-Cdh1; Clb2-ken was fully sensitive to APC-Cdc20 and reduced 13-fold in sensitivity to APC-Cdh1; and Clb2-ken,db was resistant to both versions of the APC (Wäsch and Cross, 2002).

Clb2 Overexpression Modeled in a Boolean Network Computational Cell Cycle Model

Recently, Li *et al*. (2004) presented a Boolean network computational model for the budding yeast cell cycle (Figure 7). In this model, cell cycle regulators are represented as nodes that have the values 0 (off) or 1 (on); these nodes interact with each other in successive time steps according to rules based on a highly simplified form of the circuitry used in the Chen *et al*. (2004) model. This Boolean model has the advantage that the endpoint that the network will reach can be

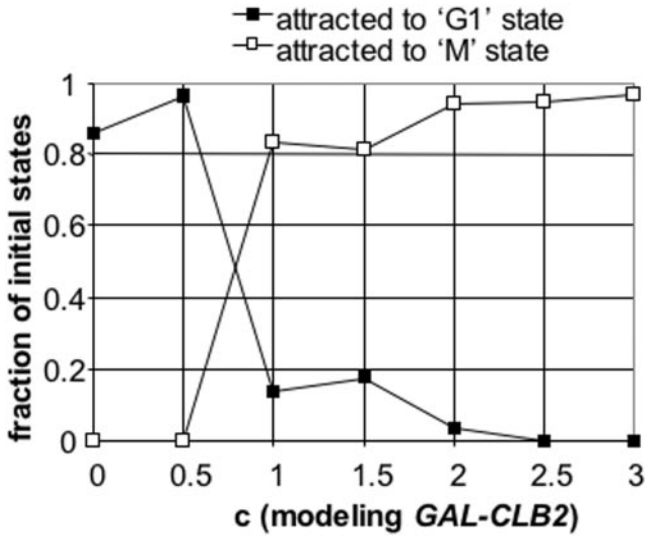

Figure 7. Boolean network predictions. The Boolean network model of Li *et al*. (2004) was implemented using Matlab software (code available on request). Equation 1 of the model was modified by adding a constant c to the Σ(aij*Sj(t)) term for the Clb2 node (j = 10). This has the effect of adding a fixed positive input to the Clb2 node. For the indicated values of c, the 2048 distinct starting configurations of the network were run until a steady state was reached. The proportions of states arriving at the G_1 state of Li *et al*. (2004), or arriving at the M-phase state 9 of Li *et al*. (2004), are plotted for each value of c.

evaluated from each of the 2048 possible starting configurations of node values. From most starting states, the network converged to a trajectory, interpretable as a normal cell cycle sequence, ending in a "G_1" state with Sic1 and Cdh1 on and all other nodes off (Li *et al*., 2004). This G_1 state attracted 86% of the starting states. (This simplified model runs down to G_1 rather than cycling, because it requires an added burst of activity in the "Cln3" node to drive cell cycle Start [Li *et al*., 2004].) Adding a level c of positive input into the Clb2 node at each time step to model constitutive Clb2 expression (see *Materials and Methods*) had the following results. If c was <1, the G_1 state was the strongest attractor as in the original model, but if c is ≥ 1, the system switched to a new very strong attractor, one of the states in the converging trajectory of Li *et al*. (2004), in which the nonzero nodes are Swi5, Cdc20/Cdc14, Sic1, Clb2, and Mcm/SFF. This state, which was not an attractor with c = 0, attracted $\geq 81\%$ of the starting states with c ≥ 1. [For c values of 1–2, almost all of the starting states that did not lead to the new attractor led instead to the original G_1 state of Li *et al*. (2004), suggesting bistability, an interesting feature of some nonlinear biological networks; Ferrell, 2002]. This state reflects a predicted activation of the mitotic exit network, signaled by Swi5, Cdc14, and Sic1 nodes being on, combined with persistence of the Clb2 and Mcm/SFF nodes that are normally inactivated by the mitotic exit network. Therefore, the state is a reasonable "M-phase" analog given the nonquantitative limitations of Boolean networks. Thus, two computational models of the cell cycle, based on very different mathematical principles, both lead to the conclusion that mitotic arrest due to sufficient constitutive Clb2 expression is a robust property of the cell cycle network, with a sharp onset at a specific level of additional Clb2 added to the system.

DISCUSSION

A Cyclin Threshold for Block of Mitotic Exit

Oscillation of mitotic cyclin abundance is critical for cell cycle regulation, because high levels are required for induction of mitotic events but low levels are required for resetting to a new cell cycle. It is remarkable, therefore, that the main mitotic cyclin Clb2 can be driven by a constitutive promoter ~10 times as active as the endogenous promoter is at its peak, without significantly reducing viability. This finding emphasizes the highly robust nature of the cell cycle control machinery. Under these conditions, though, normally dispensable regulatory components such as Cdh1 and Sic1 become essential, and the system exhibits high-dosage sensitivity for these regulators; thus, the robustness of the wild-type system is compromised at this Clb2 expression level. A twofold further increase in Clb2 expression then crosses a threshold due to inhibition of mitotic exit. It is interesting that mutual inhibition between mitotic cyclin and the Cdh1–Sic1 inhibitory system yields a potentially bistable system (Chen *et al*., 2004); such systems are commonly characterized by sharp thresholds and hysteresis (Ferrell, 2002; Pomerening *et al*., 2003; Sha *et al*., 2003).

Evaluation of a Quantitative Cell Cycle Model

The Chen *et al*. (2004) model was based for the most part on qualitative genetic observations (e.g., inviability of cells lacking all G_1 cyclins; inviability of cells expressing Clb2 lacking its destruction box from the endogenous promoter). These observations were fitted to an underlying model incorporating regulated gene expression and proteolysis, stoichiometric inhibitor binding, and a rough sense of cell biological wiring such that given levels of cyclin–Cdk activity and other regulators would yield central cell cycle events such as DNA replication and mitosis. The large number of "moving parts" in the model, and the complexity of function of each of these parts, make the model a highly complex object (although still clearly much simpler than a cell!). Although it is a significant achievement to fit the large number of mutants that the model handles, it is a concern that all of the data were used to generate the model, leaving no immediate opportunity to establish whether the model is truly predictive.

Overall, the Chen *et al*. (2004) model agrees qualitatively and quantitatively with the present results on mitotic cyclin Clb2 overexpression. The experimental observations used as constraints in model generation included no such quantitative observations, and very little quantitative biochemical data of any type. Thus, the present results are fully independent confirmation of a central aspect of the model: the sensitivity and response to high and low mitotic cyclin levels. These are central because of the ratchet-like manner in which some steps in cell cycle events are promoted, and others inhibited, by high cyclin–Cdk levels (Nasmyth, 1996); thus, it is critical that a quantitative model handle mitotic cyclin levels appropriately.

In other experiments, we have examined the ability of the model to predict levels of various components (Sic1, Cdc6, Cln2, Clb5, and Clb2) upon inactivation of mitotic cyclins *CLB1–4* or of all B-type cyclins *CLB1–6*. Reasonable quantitative agreement was found in most cases (Li and Cross, unpublished data). Such results, as well as those published previously (Cross *et al*., 2002) suggest that the model works well at predicting consequences of mitotic cyclin limitation, as well as the consequences of mitotic cyclin overexpression as reported here.

It is important to note that the results reported here certainly do not imply that the model is correct in all mechanistic detail. The cell cycle control machinery is somewhat modular; for example, the G_1 cyclin regulatory module is essentially independent from the mitotic exit network regulating Cdc14 release, except that both impinge on B-type cyclin regulation, primarily by affecting Cdh1 and Sic1 inactivation or activation (see wiring diagram and discussion in Chen *et al*., 2004). This modularity is reflected in model construction, with the consequence that the model could simulate B-type cyclin regulation with quantitative accuracy provided the G_1 cyclin regulatory module or the mitotic exit network module has approximately correct input–output relationships for a given level of B-type cyclin, even if details of the modular mechanisms are incorrect. This could explain how the model could work very well with incomplete information (for example, as noted in Chen *et al*. (2004), the model lacked explicit formulation of the FEAR pathway regulating Cdc14 release; Stegmeier *et al*., 2002). Similarly, as noted above and in Cross *et al*. (2002), a fully detailed model will have to account for the complicated pattern of mitotic cyclin partial functional redundancy, rather than simply dealing with Clb2 as a stand-in for Clb1,2,3,4.

As model development continues and confidence in the predictive accuracy of the model increases, it will be possible to place greater reliance on it as a tool for further exploration. The core cell cycle oscillator in the model can be explored as a mathematical object, with the hope of obtaining deeper insight into biological network structure and evolution, and the oscillatory mechanism can be connected up in a mechanistically accurate way to other cellular behaviors such as cell-cycle-regulated gene expression (Spellman *et al*., 1998), DNA replication, and cell morphogenesis.

ACKNOWLEDGMENTS

We thank J. Bean and E. Siggia for help with time-lapse microscopy. We also thank A. Amon, A. Murray, and K. Lee for strains and J. Tyson and E. Siggia for helpful discussions. This work was supported by Public Health Service grant GM-47238 and Defense Advanced Research Projects Agency F30602-01-2-0572.

REFERENCES

Archambault, V., Li, C. X., Tackett, A. J., Wäsch, R., Chait, B. T., Rout, M. P., and Cross, F. R. (2003). Genetic and biochemical evaluation of the importance of Cdc6 in regulating mitotic exit. Mol. Biol. Cell *14*, 4592–4604.

Chen, K. C., Calzone, L., Csikasz-Nagy, A., Cross, F. R., Novak, B., and Tyson, J. J. (2004). Integrative analysis of cell cycle control in budding yeast. Mol. Biol. Cell *15*, 3841–3862.

Chen, K. C., Csikasz-Nagy, A., Gyorffy, B., Val, J., Novak, B., and Tyson, J. J. (2000). Kinetic analysis of a molecular model of the budding yeast cell cycle. Mol. Biol. Cell *11*, 369–391.

Cross, F. R. (2003). Two redundant oscillatory mechanisms in the yeast cell cycle. Dev. Cell *4*, 741–752.

Cross, F. R., Archambault, V., Miller, M., and Klovstad, M. (2002). Testing a mathematical model of the yeast cell cycle. Mol. Biol. Cell *13*, 52–70.

Diffley, J. F., and Labib, K. (2002). The chromosome replication cycle. J. Cell Sci. *115*, 869–872.

Evans, T., Rosenthal, E. T., Youngblom, J., Distel, D., and Hunt, T. (1983). Cyclin: a protein specified by maternal mRNA in sea urchin eggs that is destroyed at each cleavage division. Cell *33*, 389–396.

Ferrell, J. E., Jr. (2002). Self-perpetuating states in signal transduction: positive feedback, double-negative feedback and bistability. Curr. Opin. Cell Biol. *14*, 140–148.

Fitch, I., Dahman, C., Surana, U., Amon, A., Nasmyth, K., Goetsch, L., Byers, B., and Futcher, B. (1992). Characterization of four B-type cyclin genes of the budding yeast *Saccharomyces cerevisiae*. Mol. Biol. Cell *3*, 805–818.

Hara, K., Tydeman, P., and Kirschner, M. (1980). A cytoplasmic clock with the same period as the division cycle in *Xenopus* eggs. Proc. Natl. Acad. Sci. USA *77*, 462–466.

Hendrickson, C., Meyn, M. A., 3rd, Morabito, L., and Holloway, S. L. (2001). The KEN box regulates Clb2 proteolysis in G1 and at the metaphase-to-anaphase transition. Curr. Biol. *11*, 1781–1787.

Iwabuchi, M., Ohsumi, K., Yamamoto, T. M., and Kishimoto, T. (2002). Co-ordinated regulation of M phase exit and S phase entry by the Cdc2 activity level in the early embryonic cell cycle. Dev. Biol. *243*, 34–43.

Li, F., Long, T., Lu, Y., Ouyang, Q., and Tang, C. (2004). The yeast cell-cycle network is robustly designed. Proc. Natl. Acad. Sci. USA *101*, 4781–4786.

Murray, A. W., and Kirschner, M. W. (1989). Cyclin synthesis drives the early embryonic cell cycle. Nature *339*, 275–280.

Murray, A. W., Solomon, M. J., and Kirschner, M. W. (1989). The role of cyclin synthesis and degradation in the control of maturation promoting factor activity. Nature *339*, 280–286.

Nasmyth, K. (1996). At the heart of the budding yeast cell cycle. Trends Genet *12*, 405–412.

Novak, B., and Tyson, J. J. (1993). Numerical analysis of a comprehensive model of M-phase control in *Xenopus* oocyte extracts and intact embryos. J. Cell Sci. *106*, 1153–1168.

Pomerening, J. R., Sontag, E. D., and Ferrell, J. E. (2003). Building a cell cycle oscillator: hysteresis and bistability in the activation of Cdc2. Nat. Cell Biol. *5*, 346–351.

Rudner, A., and Murray, A. (2000). Phosphorylation by Cdc28 activates the Cdc20-dependent activity of the anaphase-promoting complex. J. Cell Biol. *149*, 1377–1390.

Sha, W., Moore, J., Chen, K., Lassaletta, A. D., Yi, C. S., Tyson, J. J., and Sible, J. C. (2003). Hysteresis drives cell-cycle transitions in *Xenopus laevis* egg extracts. Proc. Natl. Acad. Sci. USA *100*, 975–980.

Spellman, P. T., Sherlock, G., Zhang, M. Q., Iyer, V. R., Anders, K., Eisen, M. B., Brown, P. O., Botstein, D., and Futcher, B. (1998). Comprehensive identification of cell cycle-regulated genes of the yeast *Saccharomyces cerevisiae* by microarray hybridization. Mol. Biol. Cell *9*, 3273–3297.

Stegmeier, F., Visintin, R., and Amon, A. (2002). Separase, polo kinase, the kinetochore protein Slk19, and Spo12 function in a network that controls Cdc14 localization during early anaphase. Cell *108*, 207–220.

Stern, B., and Nurse, P. (1996). A quantitative model for the cdc2 control of S phase and mitosis in fission yeast. Trends Genet. *12*, 345–350.

Stillman, B. (1996). Cell cycle control of DNA replication. Science *274*, 1659–1664.

Surana, U., Amon, A., Dowzer, C., McGrew, J., Byers, B., and Nasmyth, K. (1993). Destruction of the CDC28/CLB mitotic kinase is not required for the metaphase to anaphase transition in budding yeast. EMBO J *12*, 1969–1978.

Thornton, B. R., Chen, K. C., Cross, F. R., Tyson, J. J., and Toczyski, D. P. (2004). Cycling without the cyclosome: modeling a yeast strain lacking the APC. Cell Cycle *3*, 629–633.

Tyson, J. J., Novak, B., Chen, K., and Val, J. (1995). Checkpoints in the cell cycle from a modeler's perspective. Prog. Cell Cycle Res. *1*, 1–8.

Wäsch, R., and Cross, F. R. (2002). APC-dependent proteolysis of the mitotic cyclin Clb2 is essential for mitotic exit. Nature *418*, 556–562.

Zachariae, W., and Nasmyth, K. (1999). Whose end is destruction: cell division and the anaphase-promoting complex. Genes Dev. *15*, 2039–2058.